

Effects of Fluid Properties and System Pressure on Convective Boiling in Microtubes

Tzu-Hsiang Yen, Nobuhide Kasagi and Yuji Suzuki

Department of Mechanical Engineering, The University of Tokyo,
Bunkyo-ku, Hongo 7-3-1, Tokyo, 113-8656

ABSTRACT

An experimental investigation of convective boiling in microtubes is carried out. With ethanol, HCFC123 and FC72 being employed as a working fluid, the local heat transfer coefficient and the pressure drop are measured in 0.19, 0.3 and 0.51 mm ID tubes. It is found that the heat transfer coefficient is insensitive to the heat and mass fluxes, while strongly dependent on the inner diameter, surface roughness, system pressure and the latent heat of the working fluid. The pressure loss characteristics are similar to those in conventional-size tubes. These observations can be explained by the nucleate bubble growth in confined space.

INTRODUCTION

Highly efficient heat exchangers have become even more important because of the rapid increase of the heat dissipation rate in high-end electronic devices. Since Tuckerman and Pease [1] obtained large overall heat transfer coefficient in microchannels fabricated on a Si wafer, heat transfer research in micro conduits for both single and multi-phase flows have attracted much attention.

In the last decade, peculiar heat transfer characteristics of convective boiling have been reported in minitubes (0.6 ~ 3 mm) and microtubes (< 0.6mm, e.g., Kandlikar [2]; Mehendale et al., [3]). In microtubes, high liquid superheat phenomena were also discovered. Peng et al. [4] carried out convective subcooled boiling experiments in 200 ~ 600 μ m ID microchannels and reported that nucleation bubbles were hardly observed in the boiling regime. Recently, such high liquid superheat was attributed to the lack of active nucleate sites. However, the dominant parameters for the onset and the magnitude of the superheat are still unknown.

Since accurate measurement of temperature, pressure, heat flux and mass flow rate in a single microtube is extremely difficult, the heat transfer characteristics in microtubes of less than 1 mm ID still remains unclear. Ravigururajan [5] measured the average heat transfer coefficient in parallel microchannels of 425 μ m ID. Yen et al. [6] made a series of experiments in a single microtube of 0.19-0.51 mm ID and examined the liquid superheat and the local heat transfer characteristics in detail.

The objective of the present study is to extend the experimental study of Yen et al. [6], and obtain local heat transfer coefficients and pressure losses of convective boiling in microtubes for different refrigerants under different system pressures and surface roughness. We carried out a series of experiments on saturated convective boiling in microtubes of 0.19, 0.3 and 0.51 mm ID at low heat (1~13 kW/m²) and mass (50~350 kg/m²s) fluxes.

Experimental apparatus

Figure 1 shows the experimental loop of the microtube system [6]. A twin plunger pump (Moleh, MT-2221) was employed in most experiments in order to provide extremely low mass flux from 50 to 350 kg/m²s (about 10⁻⁵~10⁻⁶ kg/s). The uncertainty interval of the flow rate is within \pm 1%. The system pressure of the test section is controlled by a helium tank, which is connected to the pressurized working-fluid reservoir. The system pressure is measured by a diaphragm pressure transducer (Druck, PMP-1400).

Two types of the microtubes made from SUS304 stainless steel and titanium are used. Figure 2 shows SEM images of the inner surface of two different microtubes. The SUS304 surface tube has grooves of 2~3 μ m width and cavities of 4~6 μ m diameter. On the other hand, the titanium tube surface is much smoother with only grooves of 1~2 μ m width sparsely distributed.

The inner diameter of the test section was chosen as 0.51 mm, 0.3mm and 0.19 mm for SUS304, and 0.5 mm for titanium. Their outer diameter was respectively 0.81 mm, 0.51 and 0.41 mm for the SUS304 tubes and 0.7 mm for the titanium tube. The length of all the test sections is about 28cm. The pressure loss of the test section was measured by a diaphragm pressure transducer (Sokken, PZ-77-D) through inlet and outlet pressure ports.

The test section was heated by a direct current, and the heat loss to the environment was compensated [6]. Twelve K-type thermocouples of 25 μ m OD were glued onto the tube outer wall with thermally conductive silicon (k=0.9W/(mK), Shin-Etsu Silicones, KE3493). One K-type thermocouple was inserted into the inlet manifold for the measurement of the inlet fluid temperature. Cold junctions of the thermocouples were submerged into a standard temperature bath (Komatsu Electronics, Model ZC-114), in which the temperature was maintained at 0 ~ 0.02 K. Calibration of the thermocouples was made between 20 and 90 °C. Standard estimation errors of the thermocouples were within \pm 0.1 K.

Data reduction procedure

The heat loss to the environment is assumed to be as a function of the wall temperature T_{wout} . The inner wall temperature T_{win} is calculated by solving the one-dimensional heat conduction equation with the boundary conditions at the outer surface of the tube. After onset of the saturated boiling, the working fluid temperature T_{ref} is assumed to be at the saturated temperature. The saturated temperature is determined using local pressure, which is estimated by a linear interpolation of the pressure difference over the saturated region. The heat transfer coefficient is then

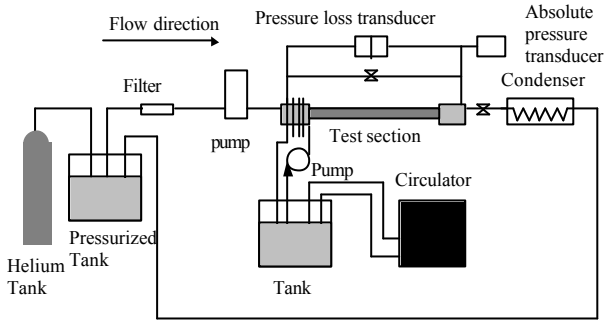


Fig. 1 Experimental loop.

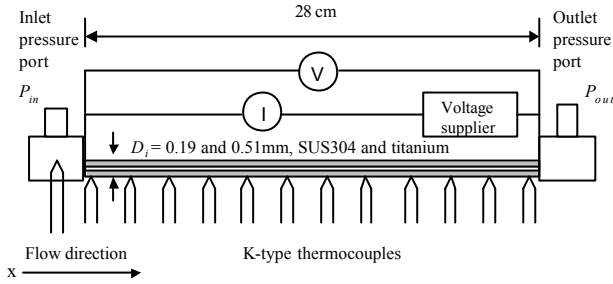
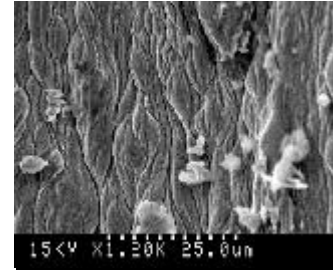
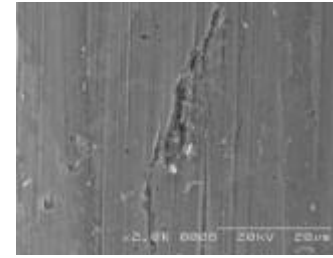


Fig. 3 Test section.



(a)



(b)

Fig. 2 SEM images of the inner surfaces of SUS304 (a) and titanium (b) test sections.

calculated as

$$h_{sat} = \frac{q}{T_{win} - T_{ref}} \quad (1)$$

Since the fluid is heated from subcooled liquid to superheated vapor states in the test section, the total pressure loss ΔP_{total} is composed of

$$\Delta P_{total} = \Delta P_{sub} + \Delta P_{sat} + \Delta P_{sup} \quad (2)$$

where ΔP_{sub} , ΔP_{sat} , and ΔP_{sup} are the pressure losses in the subcooled liquid, saturated boiling, and superheated vapor regions, respectively. The length of the subcooled region l and the pressure loss ΔP_{sub} are calculated as follows.

We first assume an arbitrary value for l , and calculate ΔP_{sub} as

$$\Delta P_{sub} = f \frac{1}{2} \rho U^2 \frac{l}{D_i} \quad (3)$$

where f , ρ and U are the friction factors of the laminar Poiseuille flow, the liquid density and the bulk mean velocity, respectively. The saturation pressure at $x = l$ is given by

$$P_{sat}(l) = P_{in} - \Delta P_{sub} \quad (4)$$

where P_{in} is the inlet pressure. Then, the saturation temperature T_{sat} is calculated from the saturation table of the refrigerant (REFPROP). Finally, the new value of l is obtained from the energy balance, i.e.,

$$\int_0^l q(x) \pi D_i dx = \dot{M} C_p (T_{sat}(l) - T_{in}) \quad (5)$$

The iterative calculation using Eqs. (3-5) is repeated until the value of l converges.

The local vapor quality χ in the saturated region is calculated as

$$\chi(x) = \frac{\int_l^x q(x) \pi D_i dx}{\dot{M} h_{lv}} \quad (6)$$

The length of the saturated region s is determined from the above integration in such a way that $\chi = 1$ at $x = l + s$. The pressure loss in the superheat region ΔP_{sup} ($l + s < x < L$) is determined by the laminar flow solution for vapor using physical properties at the local pressure and temperature.

Finally, the pressure loss in the saturated boiling region, ΔP_{sup} , is determined by Eq. (2). The local pressure $P_{sat}(x)$ in the saturated boiling region is assumed to be linearly distributed along the tube,

$$P_{sat}(x) = P_{sat}(l) - \Delta P_{sat} \frac{x-l}{s} \quad (7)$$

Experimental results

Figure 4 shows the distribution of the absolute wall temperature in the 0.19mm ID SUS304 tube when $q = 5.5 \text{ kW/m}^2$, where the wall temperature measured between $x = 0.04$ and 0.20 m is in accordance with the saturated temperature. It decreases with increasing x due to the pressure drop in the test section. Thus, conventional saturated boiling should occur under this heat flux condition. On the other hand, the wall temperature for a smaller heat flux of $q = 2.4 \text{ kW/m}^2$, monotonically increases with the axial distance and reaches $110 \text{ }^\circ\text{C}$ at $x = 0.27 \text{ m}$. The pressure drop is also in good agreement with the estimate based on the

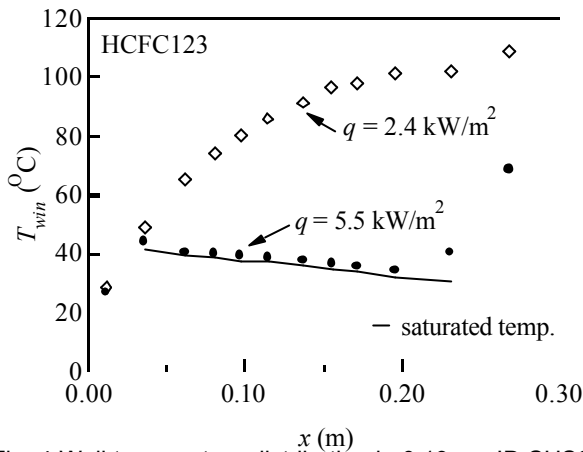


Fig. 4 Wall temperature distribution in 0.19mm ID SUS304 tube at $\dot{m} = 145 \text{ kg/m}^2 \text{ s}$.

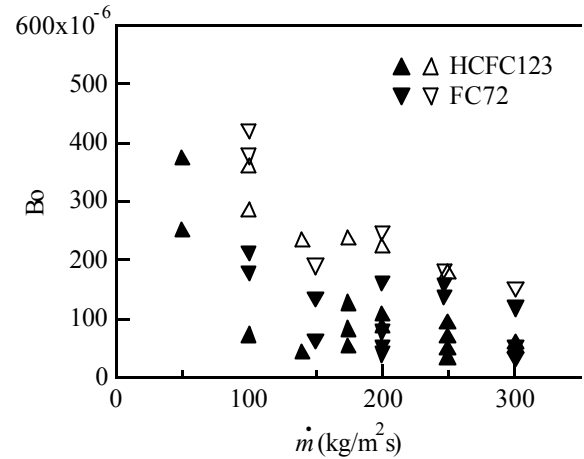


Fig. 6 Onset of liquid superheat for different refrigerants in 0.19 mm ID SUS304 tube.

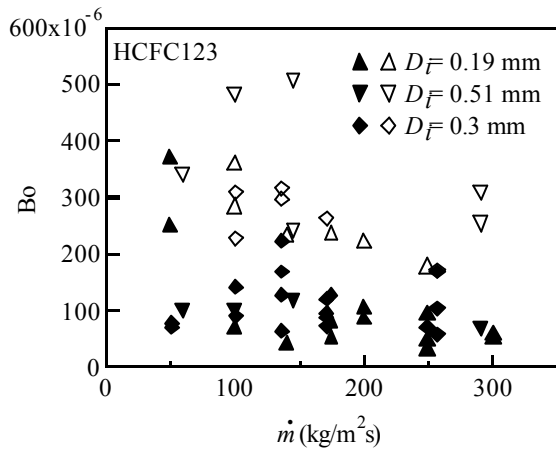


Fig. 5 Onset of liquid superheat in different inner diameter SUS304 tubes for HCFC123. Open symbols represent saturated boiling, while close symbols superheat liquid.

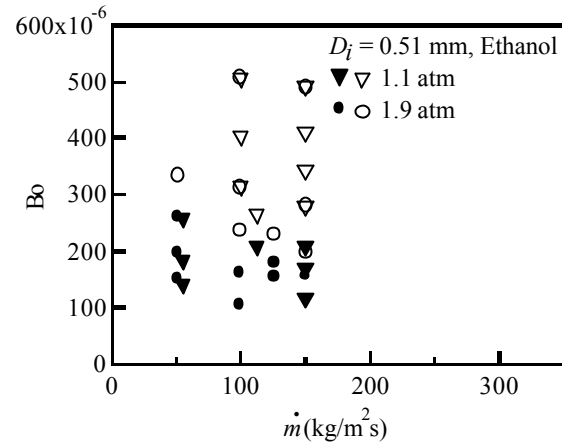


Fig. 7 Onset of liquid superheat under different system pressures in 0.51 mm ID SUS304 tube.

single-phase laminar flow [6]. Since in the single-phase flow, the temperature difference between the inner wall and the refrigerant is only $1\sim 3^\circ\text{C}$, the liquid inside the microtube under the above experimental condition should be in the superheat liquid state. This phenomenon is also observed for a stagnant fluid in micro capillaries by Brereton et al. [7]

Figure 5 shows the condition map for the superheat phenomenon as a function of the boiling number Bo and the mass flux \dot{m} . When \dot{m} is fixed, the liquid superheat occurs at smaller Bo . On the other hand, when the mass flux increases, the critical Bo for the onset of boiling decreases and seems to be independent of the tube inner diameter.

Figure 6 shows the map for FC72 and HCFC123 in the 0.19 mm ID tube. The superheat regime is almost the same for the two different refrigerants, which have different latent heats, but similar surface tension. Figure 7 shows the map for ethanol in different system pressures, the superheat region is also similar under different system pressures.

Figure 8 shows the heat transfer coefficients of HCFC123 at the same mass flux in the microtubes of

different inner diameters. The saturated boiling heat transfer coefficient decreases as the inner diameter decreases. It also decreases as the vapor quality χ is increased to $\chi = 0.3$, then remains almost constant toward $\chi = 1$. Such variation of the heat transfer coefficient is completely different from those in small or traditional-size tubes, where the convective boiling effect is dominant and the heat transfer coefficient increases with increasing χ at $\chi < 0.9$.

The decrease of the heat transfer coefficient with the increase of the vapor quality can be explained by the flow patterns in the microtube [8]. In the microtube, the main flow patterns are the slug flow and the annular flow. Partial dryout usually occurs in the local region covered by slugs. When the vapor quality increases, the length of the slug increases and the dryout region becomes larger.

Figure 9 shows the heat transfer coefficient of HCFC123 and FC72 in the 0.19 mm tube at similar mass fluxes, heat fluxes and system pressures. The heat transfer coefficient of HCFC123 is larger than that of FC72. The physical properties of HCFC123 and FC72 are similar, but HCFC123 has about two times

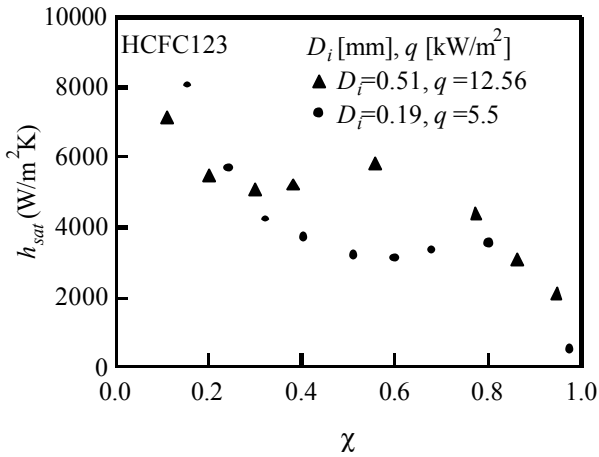


Fig. 8 Heat transfer coefficient versus vapor quality under different ID of the tube at $\dot{m}=145\text{kg/m}^2\text{s}$.

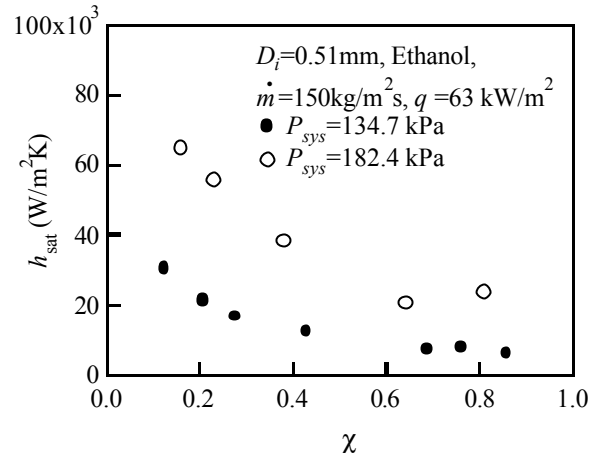


Fig. 10 Heat transfer coefficient under different system pressures in 0.51 mm ID SUS304 tube.

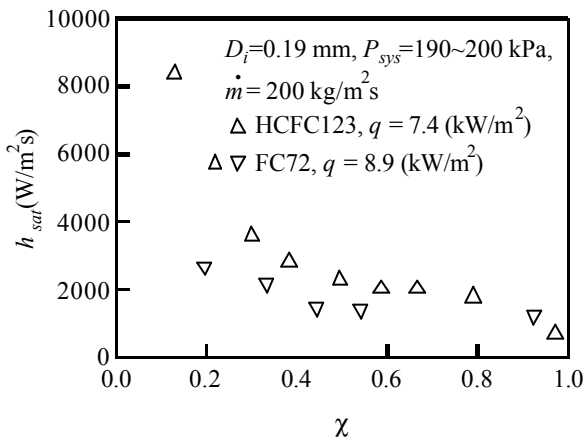


Fig. 9 Heat transfer coefficient of different working fluids in 0.19mm ID tube.

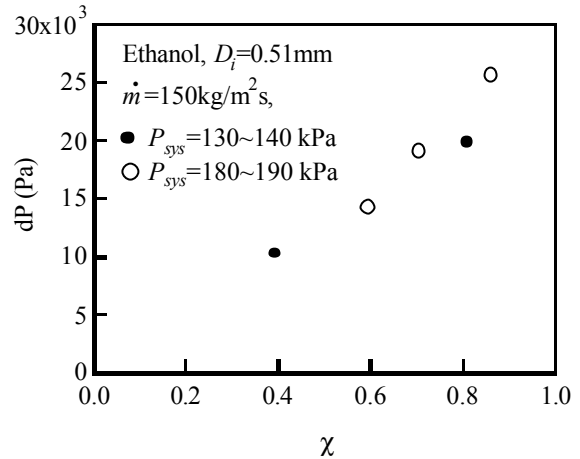


Fig. 11 Pressure loss versus vapor quality in 0.51mm ID SUS304 tube under different system pressures.

larger latent heat than FC72. Therefore, it is conjectured that, in microtubes, the heat transfer coefficient is significantly affected by the latent heat of the working fluid. This is because the evaporation in the micro layer region beneath the slug bubble is considered to be the main mechanism of the convective boiling in microtubes [8]. Thus higher latent heat of a working fluid results in higher heat transfer coefficient [9].

Figure 10 shows the heat transfer coefficient of ethanol in the 0.51mm ID tube under different system pressures. The heat transfer coefficient of ethanol is much larger than that of HCFC123 and FC72 shown in Fig. 9. Again, this is probably because the latent heat of ethanol is about 5 times larger than that of HCFC123. When the system pressure is elevated, the heat transfer coefficient also becomes larger. This phenomena can be considered as the interaction between the bubble growth and the confined space in the microtube, which will be described later.

Figure 11 shows the pressure loss of ethanol convective boiling versus the exit vapor quality in 0.51mm ID tube under different system pressures. The

effect of system pressure to the pressure loss seems to be minor.

Figure 12 shows the heat transfer coefficients of FC72 with different tubes. As shown in Fig. 2, the titanium tube has a smoother surface than SUS304. It is found that the surface roughness has a strong effect on the heat transfer coefficient. The heat transfer coefficient in the SUS304 tube (rougher surface) is about two times larger than that in the titanium tube (smoother surface). The present findings in microtubes are in accordance with previous results of convective boiling in conventional tubes [10], the number density of the cavities becomes smaller on a smoother surface.

Comparison of the heat transfer and pressure loss data to the visualization experiment

Nasu et al. [11] made a microchannel, of which hydraulic diameter is 200 μm , with the aid of the MEMS technologies. They made flow visualization of forced convective boiling under the constant heat flux condition. Figure 13 shows their flow visualization image and the conceptual schematic of the flow pattern. The flow region can be divided into three regions; the

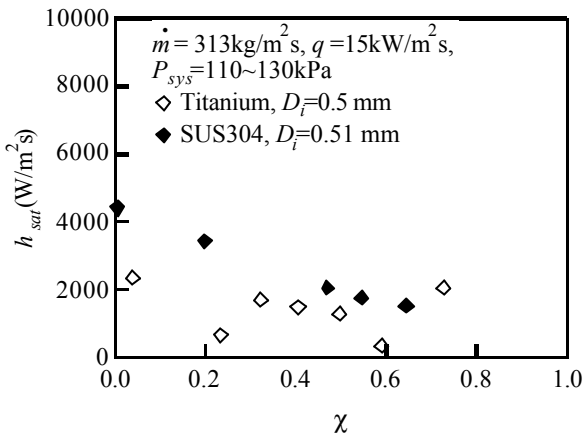


Fig. 12 Heat transfer coefficient versus vapor quality in tubes of different materials.

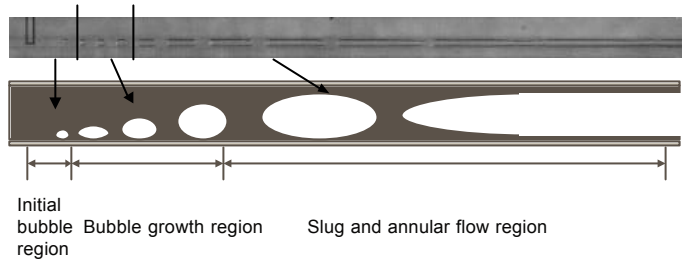


Fig. 13 An interpretation of the heat transfer mechanism of convective boiling in microtubes with reference to the flow visualization by Nasu et al. [9]

initial bubble region, the bubble growth region and the slug and annular flow region.

In the initial bubble region, the bubble is still small compared with the inner diameter of the tube. It is conjectured that this is why the onset of superheat phenomena is independent of the system pressure and tube ID. On the other hand, in the bubble growth region, the bubble diameter becomes comparable to the tube ID, and the confined space start to restrict the bubble to slug flow. Thus, the tube ID and the system pressure affects the heat transfer coefficients as described in the previous chapter. Finally, in the annular flow region, the pressure characteristics are similar to those in conventional-size tubes because nucleation becomes less important in these flow regions. Therefore, the pressure loss characteristics is similar to that in conventional tubes [6] and remains unchanged under different system pressures.

Conclusions

The heat transfer coefficient and the pressure loss of the convective boiling in microtubes were investigated using different IDs, surface roughness, and working fluids. The following conclusions can be derived:

1. The system pressure has large effect on the heat transfer coefficient. When the system pressure becomes larger, the heat transfer coefficient becomes larger.
2. Smooth surface inhibits the bubble nucleation, and the heat transfer coefficient becomes smaller.
3. According to the visualization experiment by Kandlikar [8] and Nasu et al. [11], the slug flow pattern and annular flow pattern are the main flow patterns in the convective boiling of microtubes. Thus, the peculiar heat transfer characteristics can be consistently explained by the characteristics of the slug bubble behavior in the microtube.

Nomenclature

- Bo: boiling number, $Bo=q/h_{lv}G$
- C_p : specific heat at constant pressure [J/(kg K)]
- D_o : outer diameter [m]
- D_i : inner diameter [m]

f : friction factor

\dot{M} : mass flow rate [kg/s]

\dot{m} : mass flux [kg/m² s]

h_{lv} : latent heat [J/kg]

h_{sat} : saturated boiling heat transfer coefficient [W/m K]

l : subcooled region length [m]

P_{sys} : test section pressure [kPa]

ΔP_{sub} : pressure loss over the subcooled region [kPa]

ΔP_{sup} : pressure loss over the superheated region [kPa]

ΔP_{total} : total pressure loss of the test section [kPa]

q: heat flux [W/m²]

T_{ref} : refrigerant temperature [°C]

T_{wout} : outer wall temperature [°C]

T_{win} : inner wall temperature [°C]

U: bulk mean velocity [m/s]

x: axial coordinate [m]

χ : vapor quality

ρ : liquid density [kg/m³]

References

- [1] Tuckerman, D. B., Pease, R. F. W., 1981. High-performance heat sinking for VLSI. IEEE Elec. Dev. Letters EDL-2, 126-129.
- [2] Kandlikar, S. G., 2002. Fundamental issues related to flow boiling in minichannels and microchannels, Exp. Therm. Fluid Sci. 26, 389-407.
- [3] Mehendale, S. S., Jacobi, A. M., Shah, R. K., 2000. Fluid flow and heat transfer at micro- and meso-scales with application to heat exchanger design. App. Mech. Rev. 53, 175-193.
- [4] Peng, X. F., Wang, B. -X., 1993. Forced convection and flow boiling heat transfer for liquid flowing through microchannels. Int. J. Heat Mass Transfer 26, 3421-3427.
- [5] Ravigururajan, T. S., 1998. Impact of channel geometry on two-phase flow heat transfer characteristics of refrigerants in microchannel heat exchangers, Trans ASME: J. Heat Transfer. 120, 485-491.

- [6] Yen, T.-H., Kasagi, N. and Suzuki, Y., 2003. Forced Convective Boiling Heat Transfer in Microtubes at Low Mass and Heat Fluxes, *Int. J. Multiphase Flow* 29 Issue 12, 1771-1792.
- [7] Brereton, G. J., Crilly, R. J., Spears, J. R., 1998. Nucleation in small capillary tubes. *Chem. Phys.* 230, 253-265.
- [8] Kandlikar, S.G., 2003, Flow Boiling In Microchannels: Non-Dimensional Groups And Heat Transfer Mechanisms." *Thermique et Microtechnologies Proceedings of congres de la societe Francais de la Thermique 2003*, Editors P. Marty, A. Bontemps, S. LePerson And F. Ayela, June 3-6, 2003, pp 3-21
- [9] Wayner, P. C., Kao, Y. K., and LaCroix, L. V., 1975. The Interline Heat-Transfer Coefficient of an Evaporating Wetting Film. *Int. J. Heat Mass Transfer* 19, 487-492.
- [10] Yu, J., Momoki, S. and Koyama, S., 1998. Experimental study of surface effect on flow boiling heat transfer in horizontal smooth tubes. *Int. J. Heat Mass Transfer* 42, 1909-1918.
- [11] Nasu, N., Suzuki, Y. and Kasagi, N., 2003. Fabrication of Prototype Testbench for Forced Convective Boiling in Microtube. *Proc. 40th National Heat Transfer Symp. of Japan*, Hiroshima, Japan, 357-358 (in Japanese).